J. Phys.: Condens. Matter **12** (2000) 3857–3869. Printed in the UK PII: S0953-8984(00)09393-0

Nuclear magnetic resonance study of polycrystalline $Sr_{1-x}Ca_xRuO_3$ ($0 \leqslant x \leqslant 1.0$)

M Daniel†, J I Budnick†, W A Hines†, Y D Zhang†, W G Clark‡ and A R Moodenbaugh§

† Department of Physics and Institute of Materials Science, University of Connecticut, Storrs, CT 06269-3046, USA

‡ Department of Physics and Astronomy, University of California at Los Angeles, Los Angeles, CA 90095-1547, USA

§ Department of Applied Science, Brookhaven National Laboratory, Upton, NY 11977, USA

Received 8 November 1999

Abstract. A zero-field spin-echo nuclear magnetic resonance (NMR) study of ^{99,101}Ru nuclei in polycrystalline powder samples of magnetically ordered $Sr_{1-x}Ca_xRuO_3$ ($0 \leqslant x \leqslant 1.0$) is reported. The NMR spectrum for $SrRuO_3$ at 1.3 K consists of two peaks at 64.4 MHz and 72.2 MHz corresponding to the ^{99}Ru and ^{101}Ru isotopes, respectively, and a hyperfine field of 329 kG. With the replacement of Sr by Ca, the peaks broaden somewhat, although there is essentially no change in the peak frequencies. However, the two resonance peaks show a significant reduction in height with intensity being shifted into the wings. Although electric quadrupole effects are present, the results suggest that the reduction of peak intensity when Ca is added is due mainly to a progressive loss of Ru moments participating in the magnetic ordering. The loss is a consequence of the dilution of the ferromagnetic exchange coupling between the moments. A measure of the spontaneous magnetization temperature dependence for $SrRuO_3$ ($\leqslant$21 K) has been obtained from the shift of the peak frequencies. It was found that the spontaneous magnetization decreases with a Bloch law $T^{3/2}$ temperature dependence characteristic of spin-wave excitations. From the coefficient of the temperature dependence, a value of 2.4 meV was obtained for the exchange integral which is consistent with the observed ordering temperature.

1. Introduction

3d transition-metal oxides with perovskite-based structures have received considerable attention since the discovery of high-T_c cuprate superconductivity [1]. More recently, additional interest has been stimulated by the observation of an unusually large magnetoresistance in rare-earth manganites which have potential applications in magnetic information storage and retrieval systems, and in other magnetic sensor applications [2]. Also, recent investigations have been extended to the 4d and 5d perovskite transition-metal oxides whose physical properties have, heretofore, been relatively unexplored. One important class of these oxides is the ruthenium oxides which have very interesting electronic, magnetic and structural properties. Of special note is the discovery of superconductivity in the layered ruthenate Sr_2RuO_4 [3].

In order to understand the microscopic origin of its magnetic properties, we have carried out a zero-field spin-echo nuclear magnetic resonance (NMR) study of the ^{99,101}Ru nuclei in polycrystalline samples of the ruthenate system $Sr_{1-x}Ca_xRuO_3$ ($0 \leqslant x \leqslant 1.0$). The striking difference in the magnetic properties of the isoelectronic and isostructural end members,

0953-8984/00/163857+13$30.00

$SrRuO_3$ and $CaRuO_3$, make this particular solid solution system very interesting [4–7]. Both $SrRuO_3$ and $CaRuO_3$ have a $GdFeO_3$-type orthorhombically distorted perovskite structure with a *Pbnm* space group [8–10]. $SrRuO_3$, with an ordering temperature of $T_c = 160$ K, is the only known 4d transition-metal oxide which is ferromagnetic. Values have been reported for the ordered Ru magnetic moment in the ferromagnetic phase which range from 0.8 to 1.6 μ_B, although the magnetization has not reached saturation for the highest fields utilized [11]. $SrRuO_3$ also exhibits metallic-like conductivity with a behaviour that is characterized as a 'bad metal' [12]. With the substitution of Ca for Sr, the metallic-like conductivity is maintained while the magnetic ordering temperature is suppressed [6, 7]. The suppression of the magnetism is not expected since in both Sr and Ca, the outer s and p bands are assumed to form a filled valence band and an empty conduction band that are far removed in energy from the Fermi level. The $CaRuO_3$ end member of this system has a distorted perovskite structure with a larger rotation of the RuO_6 octahedra than in $SrRuO_3$ [10]. $CaRuO_3$ is also metallic-like; however, its magnetic ground state has been a little more controversial. Early magnetization work reported evidence for antiferromagnetic order with a Néel temperature $T_N \approx 110$ K [5]; however, a later Mössbauer study by Gibb *et al* [13] has indicated a lack of long range magnetic order. For $Sr_{1-x}Ca_xRuO_3$, Curie–Weiss fits to the magnetic susceptibility in the paramagnetic state above the ordering temperature yield nearly constant values for the Ru moment consistent with the four Ru $4d^4$ electrons in the triplet (t_{2g}) ground state ($S = 1$, moment magnitude $= 2.8\,\mu_B$) [6, 7]. In spite of the Curie–Weiss behaviour in the paramagnetic state, very recent work suggests that $Sr_{1-x}Ca_xRuO_3$ is in fact an itinerant system [12].

2. Experimental apparatus and procedure

Polycrystalline powder samples of $Sr_{1-x}Ca_xRuO_3$, with $x = 0$, 0.10, 0.25, 0.50, 0.75 and 1.00, were prepared from Johnson–Matthey ruthenium oxide hydrate powder and the reagents calcium carbonate and strontium carbonate. The appropriately weighed powders were thoroughly ground together, placed into alumina boats and reacted in one atm of air at 1000 °C for 12 h. The samples were reground and heat treated at 1100 °C, followed by a second regrinding and heat treatment at 1150 °C. The two heat treatments were also carried out in one atm of air for 12 h. The powder samples were characterized using x-ray diffraction (XRD) with a Phillips Norelco diffractometer and Cu Kα radiation ($\lambda = 1.5418$ Å). In addition, magnetization measurements were carried out on a Quantum Design SQUID magnetometer for temperatures 5 K $\leqslant T \leqslant$ 315 K and magnetic fields $0 \leqslant B \leqslant 50$ kG.

Two distinct series of nuclear magnetic resonance (NMR) experiments were carried out in this work. In the first series of experiments (carried out at UConn), detailed spectra were obtained at 1.3 K for the ^{99,101}Ru nuclei in $Sr_{1-x}Ca_xRuO_3$ over the range of composition $0 \leqslant x \leqslant 0.75$. ($CaRuO_3$, the $x = 1.00$ composition, does not exhibit a magnetic ordering down to 1.3 K and, consequently, has no zero-field spin-echo NMR signal.) The zero-field spin-echo NMR spectra were obtained over the frequency range from 50 to 80 MHz using a commercially available Matec model 5100 mainframe and model 525 gated RF amplifier in combination with a model 625 broadband receiver with phase sensitive detection. The NMR signals were optimized using a standard spin-echo pulse sequence with RF pulses ranging from 0.6 to 1.0 μs, a pulse separation of 20 μs and a repetition rate of 20 Hz. Useable spectra were obtained by averaging the NMR signals 500 to 2000 times at 0.20 MHz intervals across the spectrum. A temperature of 1.3 K was obtained by pumping on liquid He in a conventional double Dewar system. The reader is referred to Zhang *et al* [14] and references therein for details concerning the pulsed NMR apparatus, experimental procedure, and data acquisition and analysis.

In the second series of experiments (carried out at UCLA), the temperature dependence of the ^{99,101}Ru NMR peaks for $SrRuO_3$ was carefully measured over the temperature range for which useable signal could be detected, 2.7 to 21 K. The zero-field spin-echo NMR spectra were obtained for frequencies spanning both isotopes using a laboratory-built heterodyne spectrometer and a He gas-flow cryostat that was placed in a He storage dewar. The NMR signals were obtained by averaging 256 times at 0.20 MHz frequency intervals across the spectrum. It was found that a careful tuning of the NMR probe at each operating frequency was crucial to eliminate undesirable experimental artifacts. The final absorption spectra were obtained by applying the fast Fourier transform (FFT) to the full echo, optimizing the phase, shifting the transformed signal by the corresponding frequency, and summing the result (FSS method) [15]. A Hamming filter window was applied to each transient prior to the FFT operation to remove noise away from the individual signals before frequency shifting and summing the spectra.

In the NMR measurements, it was somewhat difficult to establish the optimal excitation conditions, i.e. pulse amplitude and duration, for obtaining the spectra. This is attributed to the large ferromagnetic enhancement factor $\eta = B_{1\ eff}/B_{1\ appl}$ (response of the domain wall magnetization to the RF magnetic field) and its spatial variation in the magnetic state of the material. The variation in the enhancement factor gives rise to a significant variation in tipping angle by the RF pulses used to generate the NMR spin echoes. In particular, it was observed that the spin-echo height was a broad function of the tipping angle. Furthermore, it was observed that conditions corresponding to relatively large tipping angle resulted in anomalous echo shapes and multiple echoes [16]. By using relatively short, small amplitude RF pulses, this distortion of the echo shape could be substantially reduced without reducing the size of the signal. Such low power excitation conditions have been shown to produce reliable NMR spectra [14]. A detailed discussion concerning the enhancement factor and the effects of pulse amplitude and duration on the NMR spin-echo wave form is available in the literature [14, 16, 17].

3. Results and analysis

The polycrystalline powder samples were characterized using both XRD and magnetization. Figure 1 shows the orthorhombic lattice parameters a, b and c, which were obtained by fitting the XRD peaks for $Sr_{1-x}Ca_xRuO_3$ over the range of composition $0 \leqslant x \leqslant 1.00$. Within the limits of detectability, the XRD patterns did not indicate the presence of any second phase or any evidence of a superstructure. The low field magnetization measurements did, however, indicate the presence of a relatively small amount of $SrRuO_3$ second phase in the Ca-substituted samples (see below). As expected from atomic size considerations, there is a general decrease in the volume per formula unit with the replacement of Sr by Ca. Furthermore, as Ca is added, splitting of the main peak (consisting of the (200), (020) and (112) reflections) becomes more pronounced indicating a progressive increase in the distortion from tetragonal to orthorhombic symmetry. The magnetization results, summarized in table 1, include parameters from the ferromagnetic state below the ordering temperature as well as from the paramagnetic state above the ordering temperature. For the various compositions, table 1 lists the magnetic ordering temperature, T_c, and magnetically ordered moment (component) per Ru atom, μ_z/Ru, at the lowest temperature (5 K) and highest field (50 kG) available. In addition, above T_c and over the temperature range 215 K $\leqslant T \leqslant$ 315 K fits of the paramagnetic susceptibility were made to the Curie–Weiss law

$$\chi(T) = \frac{N\mu_{eff}^2}{3k_B(T-\Theta)} + \chi_0 \tag{1}$$

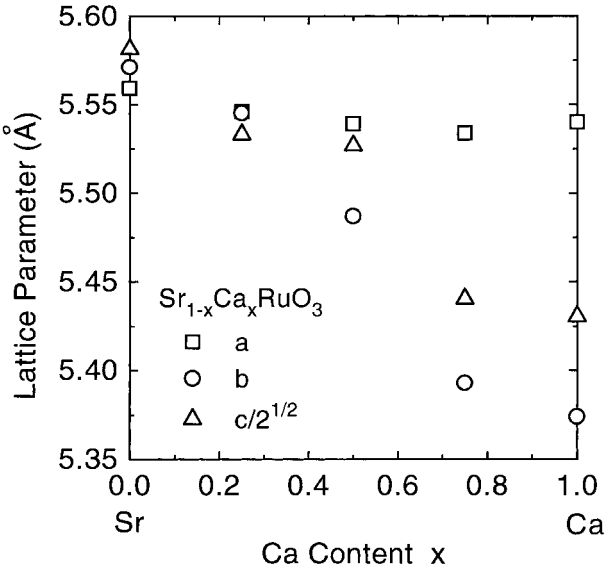

Figure 1. Orthorhombic lattice parameters a, b and $c/\sqrt{2}$ obtained from fits of the XRD patterns for polycrystalline powder $Sr_{1-x}Ca_xRuO_3$ versus the Ca content. The error in the measurements is represented by the size of the data symbols.

Table 1. Magnetic properties of $Sr_{1-x}Ca_xRuO_3$.

x	T_c (K)[a]	μ_z/Ru(μ_B)[a]	Θ (K)[b]	μ_{eff}(μ_B)[b]
0	160	1.3_4	160	2.7_7
0.25	89	0.87	126	2.6_7
0.50	53	0.42	47	2.8_5
0.75	38	0.23	0.5	2.8_4
1.00	—	—	−138	2.9_2

[a] Parameters obtained from the magnetization in the magnetically ordered state.
[b] Parameters obtained from Curie–Weiss fits to the magnetization in the paramagnetic state.

where N is the concentration of Ru moments, μ_{eff} is the effective Ru moment (magnitude), k_B is the Boltzmann constant, Θ is the Curie–Weiss temperature and χ_0 is a temperature independent term which reflects the core diamagnetism, Landau diamagnetism and Pauli paramagnetism. The parameters obtained from the Curie–Weiss fits, μ_{eff} and Θ, are also listed in table 1. Below the ordering temperature, for the compositions $0 \leqslant x \leqslant 0.75$, the magnetic behaviour is characterized by hysteresis with considerable remanence and coercive field, but a lack of saturation at the highest field. The bulk structural and magnetic characteristics observed for the polycrystalline samples used in this work are completely consistent with earlier results [6, 7, 10]. Finally, it should be noted that measurements of both the zero-field-cooled and field-cooled temperature dependence of the magnetization for low magnetic field ($\approx$30 gauss) revealed a small amount of $SrRuO_3$ second phase (characterized by the 160 K ordering temperature) in the Ca-doped samples. This was most clearly distinguishable in the $Sr_{0.25}Ca_{0.75}RuO_3$ sample where the amount of second phase is estimated to be $\leqslant$2.5%. As the $SrRuO_3$ phase has a tendency to precipitate, this is a difficult and common problem in the preparation of polycrystalline samples involving Sr and Ru [18].

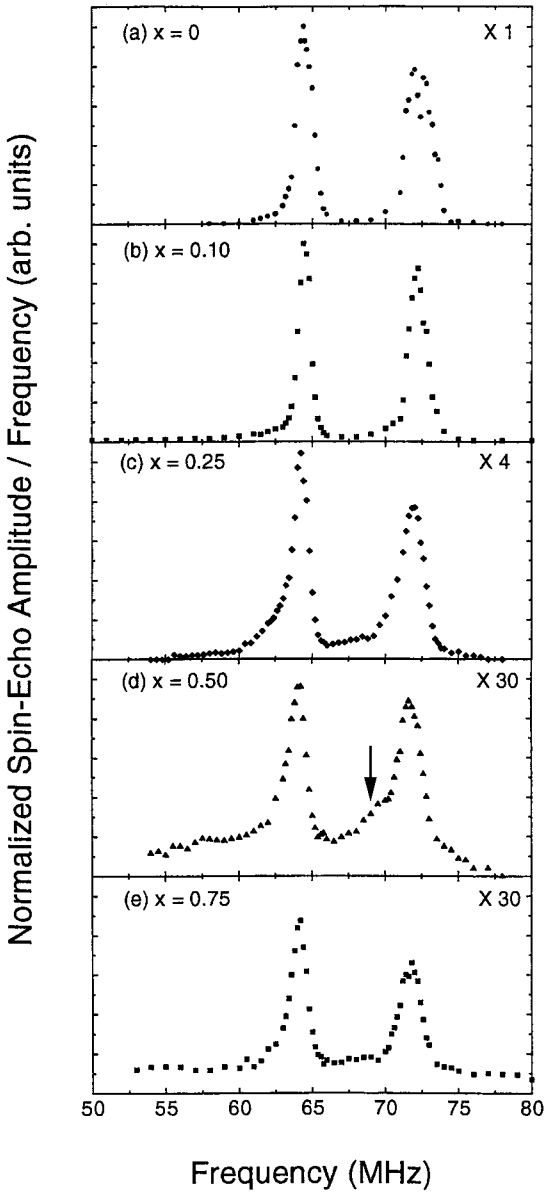

Figure 2. ^{99,101}Ru zero-field spin-echo NMR spectra obtained at 1.3 K for polycrystalline powder $Sr_{1-x}Ca_xRuO_3$: (a) $x = 0$, (b) $x = 0.10$, (c) $x = 0.25$, (d) $x = 0.50$ and (e) $x = 0.75$. For a comparison of the signal intensities (spin-echo amplitudes), the factor by which each spectrum has been multiplied is provided in the upper right-hand corner. For each composition, the horizontal line at the bottom indicates zero spin-echo amplitude. The arrow in figure 2(d) indicates the appearance of electric quadrupole structure near the peak.

Figure 2 shows the zero-field spin-echo NMR spectra obtained at 1.3 K for the polycrystalline $Sr_{1-x}Ca_xRuO_3$ samples with compositions $x = 0$, 0.10, 0.25, 0.50 and 0.75. In order to directly compare the spin-echo amplitudes for the various compositions, a factor (indicating the amount by which the height has been multiplied) is provided in the upper

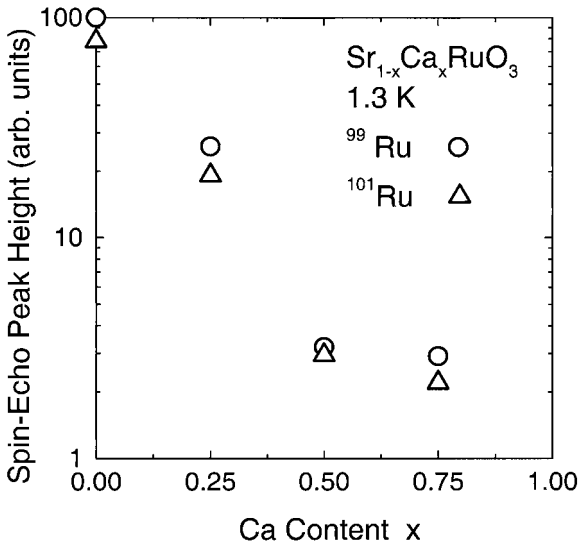

Figure 3. ^{99,101}Ru NMR signal intensity (peak height) for polycrystalline powder $Sr_{1-x}Ca_xRuO_3$ at 1.3 K versus the Ca content.

right-hand corner for each spectrum. A reliable quantitative comparison for the $x = 0.10$ composition was not possible as it had a significantly different sample mass, coil geometry and filling factor. The NMR spectrum for $SrRuO_3$ at 1.3 K consists of two peaks at 64.4 MHz and 72.2 MHz corresponding to the ^{99}Ru ($\gamma = 0.196\,45$ MHz kG^{-1}, $I = 5/2$ and 12.7% abundance) and ^{101}Ru ($\gamma = 0.220\,18$ MHz kG^{-1}, $I = 5/2$ and 17.1% abundance) isotopes, respectively [19], and a hyperfine field (HF) of 329 kG. With the replacement of Sr by Ca, the peaks at 1.3 K broaden somewhat, although there is essentially no change in the peak frequencies. There is significant decrease in the peak heights (see figure 3), which appears to be due in part to intensity being shifted away from the peaks and into the wings. Shoulder-like features are seen to appear, particularly for the ^{101}Ru peak of the $x = 0.50$ composition (indicated by the arrow in figure 2(d)). The spectral features near the peaks are consistent with a quadrupole interaction and with the fact that the replacement of the Sr atoms by Ca atoms increases the distortion of the crystal structure and increases the electric field gradient. In order to obtain a quantitative measure of the quadrupole interaction, detailed measurements of the spin-echo amplitude modulation were carried out (see below).

Figure 4 shows the variation of NMR spin-echo amplitude at the peak frequency as a function of the separation between the two RF pulses for ^{99}Ru (figure 4(a)) and ^{101}Ru (figure 4(b)) obtained from polycrystalline $SrRuO_3$ at 1.3 K. A modulation of the spin-echo amplitude is observed for both isotopes with a period of $\tau_m = 26$ μs and 4.5 μs for ^{99}Ru and ^{101}Ru, respectively. As described above, the modulation is attributed to the quadrupole interaction resulting from the deviation of the electric field gradient from cubic symmetry at the Ru sites. A theoretical treatment of the modulation has been provided by Abe *et al* [20], and the quadrupole splitting frequency can be obtained using $\Delta\nu_Q = 1/\tau_m$. The data from figure 4 yield values of $\Delta\nu_Q = 38$ and 220 kHz for ^{99}Ru and ^{101}Ru, respectively. Since the quadrupole splitting frequency $\Delta\nu_Q$ actually depends on the angle between the (internal) magnetic field and the crystalline c-axis, the quadrupole frequency ν_Q is a less ambiguous measure of the electric quadrupole interaction [21]. Measurements of the magnetization on single crystals indicate that the easy axis lies in the plane perpendicular to the c-axis [11] and,

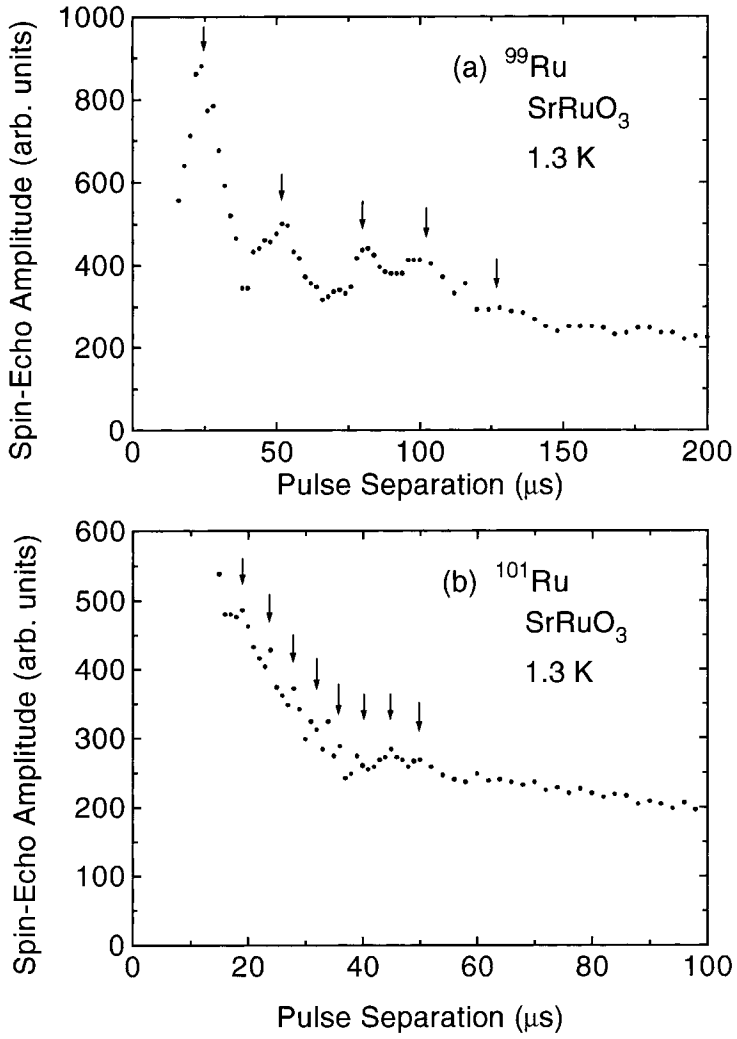

Figure 4. NMR spin-echo amplitude at the peak frequency versus the separation between the two RF pulses for $SrRuO_3$ at 1.3 K: (a) ^{99}Ru and (b) ^{101}Ru. The modulation of the spin-echo amplitude (indicated by the arrows) is attributed to the electric quadrupole interaction.

therefore, $\nu_Q = 2\Delta\nu_Q$. ν_Q can be related to the electric field gradient component $V_{zz} = eq$ and the nuclear quadrupole moment Q by the relation

$$\nu_Q = \frac{3eQV_{zz}}{2I(2I-1)h} \tag{2}$$

where I is the nuclear spin, e is the electronic charge (magnitude) and h is Planck's constant. Since V_{zz} is common for the two nuclei and both nuclei have the same spin $I = 5/2$, the ratio of the quadrupole frequencies should be equal to the ratio of the electric quadrupole moments. From the discussion above, $\nu_Q(^{101}\text{Ru})/\nu_Q(^{99}\text{Ru}) = 5.8$. Using values for the electric quadrupole moments of 0.079 and 0.457 barns (10^{-24} cm^2) for ^{99}Ru and ^{101}Ru, respectively [22], a ratio of 5.8 is calculated which is consistent with the frequency ratio. This result clearly establishes the presence of the electric quadrupole interaction. For comparison,

Table 2. Electric quadrupole frequencies, ν_Q, obtained from the spin-echo amplitude modulation.

x	^{99}Ru (kHz)	^{101}Ru (kHz)
0	77	440
0.25	200	—
0.50	250	—
0.75	660	—

it is interesting to note that direct measurements of the electric quadrupole splitting in the NMR spectra of paramagnetic Sr_2RuO_4 above the superconducting transition temperature yield values of $\nu_Q = 0.58$ and 3.3 MHz for ^{99}Ru and ^{101}Ru, respectively, having a ratio of 5.7 [23]. When the Sr atoms are replaced by the Ca atoms in $Sr_{1-x}Ca_xRuO_3$, the deviation from cubic symmetry is increased even further, which is reflected in V_{zz}, and hence, ν_Q increases. This is clearly demonstrated by the values for ^{99}Ru listed in table 2. Unfortunately, since the quadrupole moment for ^{101}Ru is so large, any addition of Ca atoms increases ν_Q to such an extent that measurement of the spin-echo modulation is inhibited.

The quadrupole effects reported here are particularly significant. It is well known that the steady state NMR signal for a nuclear species with spin I consists of $2I$ equally spaced quadrupole satellite lines with a separation $\Delta\nu_Q$. (This assumes, of course, a relatively small electric quadrupole interaction and approximately cylindrical symmetry, which is the case here.) In cases where the NMR line width is relatively narrow, $\Delta\nu_Q$, and hence ν_Q, can be obtained directly from the splitting. The results from this work demonstrate the possibility of measuring $\Delta\nu_Q$ using a pulsed NMR method in cases where the line width is inhomogeneously broadened to the extent that it exceeds $\Delta\nu_Q$, making a direct steady state NMR measurement impossible [20].

Figure 5 shows the zero-field spin-echo ^{99}Ru NMR spectra obtained for the polycrystalline $SrRuO_3$ sample at temperatures $T = 4.9$, 10.9 and 15.2 K. In this case, the normalization corresponds to setting the maximum of the spectrum equal to one. Comparison with the dashed vertical lines that indicate the centre of the two peaks at 4.9 K shows a shift to lower frequency with increasing temperature that reflects the temperature dependence of the ^{99,101}Ru HF in ferromagnetic $SrRuO_3$. One other feature that is evident from figure 5 is that the height of the ^{99}Ru peak is larger than that of the ^{101}Ru at the lowest temperature; however, it becomes smaller as T is increased. Also, as T is increased, the ^{99}Ru peak experiences a broadening such that there is substantially less change in the ratio of the spectral intensities for the two isotopes as obtained from the area under the absorption signal. The ratio of the spectral intensities is consistent with the spins, gyromagnetic ratios and abundances for the two isotopes.

A quantitative evaluation of the temperature dependence of the HF is shown in figure 6 where the fractional change in frequency ($\Delta\nu/\nu_0$) is plotted as a function of T. For this analysis, the point at which the integral of the absorption is 50% of its maximum value has been used as a criterion to determine the centre of the peak. The estimate of the error in this determination ($\pm 0.17\%$) is based on the linewidth and signal-to-noise ratio. The scatter of the data points at each temperature is consistent with this estimate. The solid line, which agrees with the data within the estimated error is given by

$$\frac{\Delta\nu}{\nu_0} = -AT^{3/2} \tag{3}$$

where $A = 1.4 \times 10^{-4}$ K$^{-3/2}$ is a coefficient chosen to fit the data in figure 6 for $SrRuO_3$. For comparison, the temperature dependence of the bulk magnetization for $SrRuO_3$ was measured at a field of 10 kG. Although the magnetization is not saturated for 10 kG, it was found that the

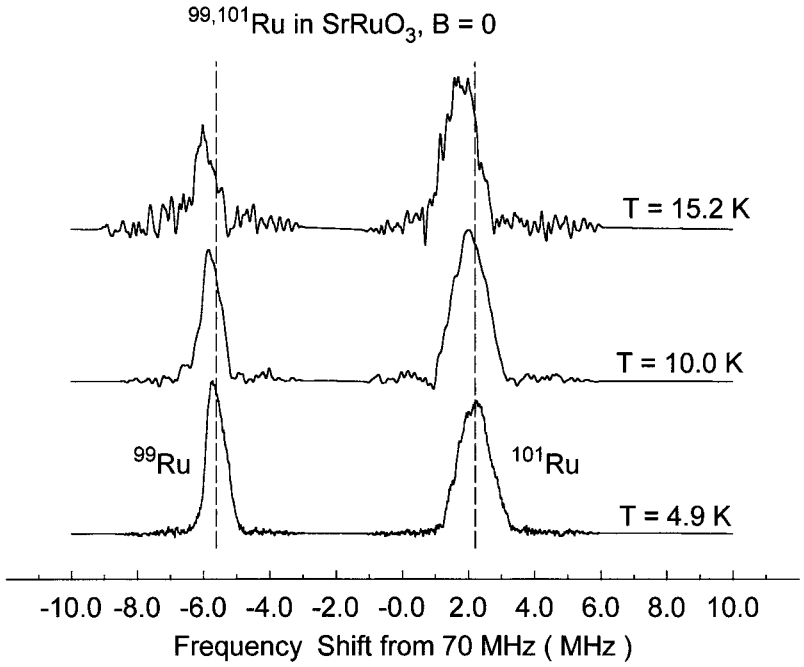

Figure 5. ^{99,101}Ru zero-field spin-echo NMR normalized absorption spectrum versus the frequency at three temperatures in $SrRuO_3$. The dashed vertical lines indicate the centre of the signal at 4.9 K.

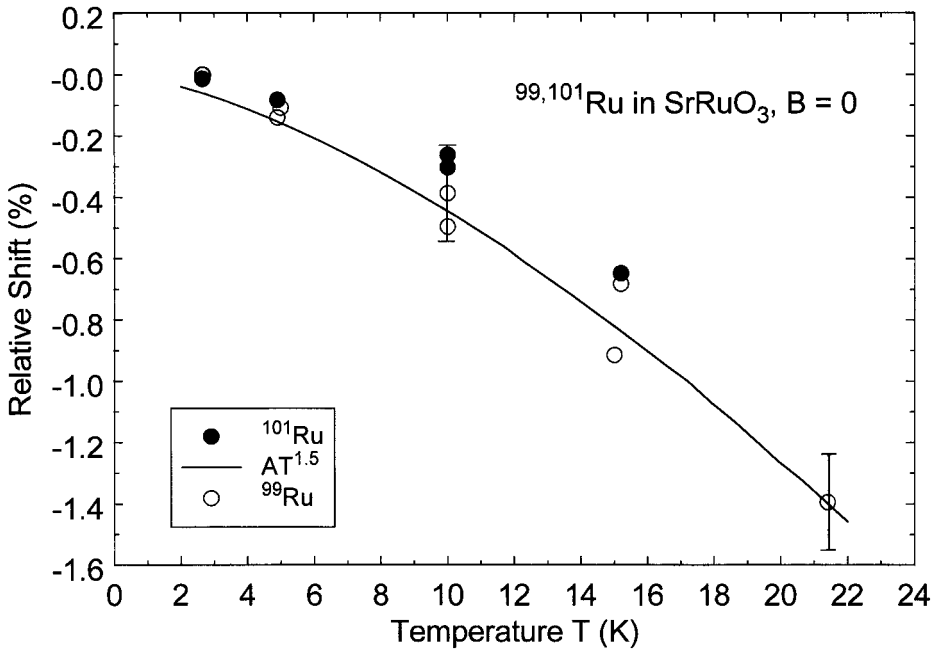

Figure 6. Relative shift of the HF for ^{99,101}Ru in $SrRuO_3$ versus the temperature. The solid line is a fit to the temperature dependence.

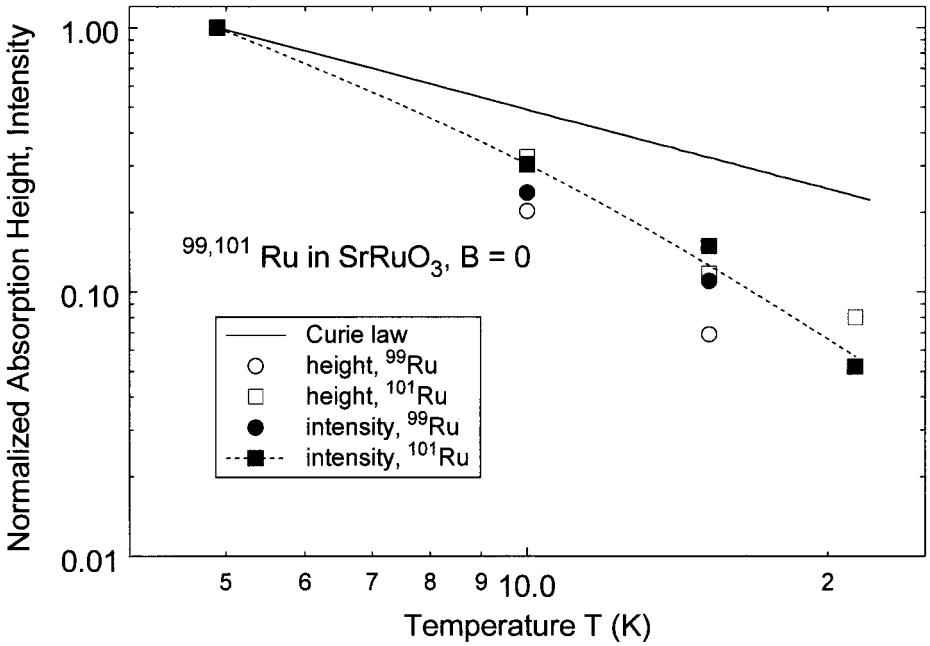

Figure 7. Normalized Ru NMR absorption height and intensity (area of the absorption) versus the temperature. The solid line is the Curie law for the nuclear magnetization and the dashed line serves as a guide for the eye for the ^{101}Ru intensity.

fractional change $\Delta M/M_0$ is also characterized by a $T^{3/2}$ temperature dependence up to 115 K (0.72 T_c) with a coefficient of 2.5×10^{-4} K$^{-3/2}$. From their magnetization measurements on thin films of $SrRuO_3$, Klein *et al* [12] report a dominant $T^{3/2}$ contribution and list a value of 1×10^{-4} K$^{-3/2}$ for the coefficient.

Finally, it was observed that the absorption signal decreased with increasing temperature substantially faster than one would expect on the basis of the Curie law (magnetization $\propto 1/T$) for the nuclear magnetization. (In this discussion, the change in the HF with T is neglected as it is too small to be a significant factor.) The temperature dependence of the absorption, normalized to the value at 4.9 K for the height of the absorption line and the integral of the absorption (spectral intensity), is shown in figure 7. The solid line is the Curie law and the dotted line is a smooth fit to the ^{101}Ru intensity. Although there is some scatter in the data, it is clear by both measures that the signal intensity falls significantly faster than the Curie law, amounting to an extra factor of four over the temperature range 5 to 20 K. It is speculated that this behaviour is related to the properties of the NMR enhancement factor η in $SrRuO_3$.

4. Discussion and conclusions

This report presents a detailed observation of the ^{99,101}Ru NMR in a magnetically ordered ruthenate oxide, $SrRuO_3$, and opens the way for further study of the complex magnetic and electronic behaviour of these systems. From the peak frequencies for the two isotopes, a HF value of 329 kG is obtained for the one crystallographic Ru site in $SrRuO_3$. This result is in complete agreement with the ^{99,101}Ru HF value obtained for $SrRuO_3$ very recently in an NMR study of a series of ruthenium oxides and Ru metal by Mukuda *et al* [25]. In the early

Mössbauer work by Gibb *et al* [13], a value of 352 kG was determined from the 5.2 → 3.2 nuclear transition for ^{99}Ru. A likely explanation for much of this discrepancy is that at the time of the Mössbauer work, the value for the ^{99}Ru nuclear moment, and consequently the gyromagnetic ratio, was not well known. During that time period, the accepted literature value was $\gamma = 0.19$ MHz kG^{-1} [24], about 3.3% smaller than the present day value of $\gamma = 0.196\,45$ MHz kG^{-1}. This would result in an overestimate for the HF of 11 kG which is slightly more than half of the discrepancy cited above. Another possible explanation is that, due to the NMR enhancement factor, the zero-field NMR signal from a multidomain powder sample originates principally from nuclei in the domain walls, whereas Mössbauer signals tend to be dominated by nuclei within the domains. This distinction must also be kept in mind when the two microscopic probes of the HF, NMR and Mössbauer effect, are used to monitor the temperature dependence of the spontaneous magnetization (see below).

When the Sr atoms are replaced by the smaller (isoelectronic) Ca atoms to form the solid solution system $Sr_{1-x}Ca_xRuO_3$, there is a general increase in the distortion of the perovskite structure along with a larger rotation of the RuO_6 octahedra. The ^{99,101}Ru NMR peaks broaden somewhat, although there is essentially no change in the peak frequencies. However, there is a significant reduction in height with intensity being shifted into the wings. Since both isotopes have nuclear spin $I = 5/2$ and the Ru site is characterized by a less-than-cubic symmetry, the strength of the electric quadrupole interaction was determined by measurements of the spin-echo amplitude modulation. From the values of ν_Q listed in table 2, it can be seen that the quadrupole interaction might possibly be responsible for structural features near the peaks; however, it cannot account for the significant transfer of intensity from the peaks to the distant wings. As an upper limit for the quadrupole broadening, the value for ν_Q for the ^{101}Ru peak in the spectrum $Sr_{0.50}Ca_{0.50}RuO_3$ can be inferred from the ^{99}Ru peak values by a simple scaling to account for the variation in V_{zz} i.e. 440 kHz × (250 kHz/77 kHz) = 1.4 MHz. This value is comparable to the peak halfwidth.

A possible explanation for the significant transfer of intensity from the peaks to the wings can be found in a phenomenological model presented by Gibb *et al* [13] to explain their Mössbauer results. In that model, they suggest that the HF at any given Ru site, Ru_i, will be proportional to $\langle S_i^z \rangle$, where the maximum value of this average spin component is $S = 1$. Furthermore, they assume that the value of $\langle S_i^z \rangle$ is proportional to the strength of the exchange interactions with six other Ru atoms, Ru_j, and that substitution of Ca for Sr reduces the exchange energy which can be written

$$E = -\sum_{j=1}^{6} J_{ij} \langle \vec{S}_i \vec{S}_j \rangle \tag{4}$$

where J_{ij} is the exchange integral for the coupled Ru spins. (In the idealized perovskite structure, each Ru atom is coupled by an Ru–O–Ru 'superexchange' to six other Ru atoms (third-nearest neighbours) with a bond angle of 180° [13]. The intermediate O atoms (first-nearest neighbours) are in the face centres of a body-centred cube with eight Sr/Ca atoms (second-nearest neighbours) at the corners.) If the spins are uncoupled, then $\langle \vec{S}_i \vec{S}_j \rangle$ will be zero; however, if the spins are strongly coupled, then $\langle \vec{S}_i \vec{S}_j \rangle$ can be taken to be one. As an approximation, they take E to be proportional to $\sum_j J_{ij}$. As each Ru–O–Ru superexchange takes place through a cube face containing four Sr/Ca atoms, it is possible to define six exchange integrals, and therefore six exchange energies, for the six possible Sr/Ca second-nearest neighbour configurations on the face. Consequently, the HF at Ru_i will be proportional to the total moment at the site, and this is taken as a linear function of the total exchange energy. With the above simplifications, Gibb *et al* [13] find that the observed HF at a Ru site will decrease by a constant increment ΔHF for every Sr atom that is replaced by a Ca atom.

From a fit of their Mössbauer data, they find that ΔHF is nearly constant with an average value of 46 kG which would shift the ^{99,101}Ru NMR peaks downward by approximately 9.2 MHz for every Sr atom that is replaced by a Ca atom. Assuming a completely random substitution of Ca for Sr, the probability of a Ru atom having n Ca second-nearest neighbours in $Sr_{1-x}Ca_xRuO_3$ is given by the binomial distribution

$$P_n(x) = \frac{8!(1-x)^{8-n}x^n}{(8-n)!n!}. \tag{5}$$

Using equation (5), the percentage of Ru atoms having zero Ca second-nearest neighbours, and therefore still contributing to the NMR peak intensity is 100%, 10%, 0.4% and ≈ 0 for $x = 0, 0.25, 0.50$ and 0.75, respectively. As shown in figure 3, the peak intensity does decrease rapidly with the Ca concentration; however, not as rapidly as predicted by equation (5). It has been suggested by Kanbayasi [6] that the substitution of Ca for Sr is not random. In addition, a significant contribution to the peaks in the spectra for the $x = 0.50$ and 0.75 compositions is likely to arise from the $SrRuO_3$ second phase. Nevertheless, it is clear that the presence of Ca in the second-nearest neighbour shell of an Ru atom causes a dramatic shift of intensity from the NMR peaks to the distant wings. In the light of earlier Mössbauer results, the NMR results presented here are consistent with a progressive loss of Ru moments participating in the magnetic ordering with the addition of Ca due to the dilution of the ferromagnetic exchange coupling between the moments. For the $Sr_{1-x}Ca_xRuO_3$ system, the magnetic coupling appears to be very sensitive to small perturbations in the Ru–O–Ru bond angle and chemical nature of the bond.

In this report, a measure of the temperature dependence for the spontaneous magnetization in $SrRuO_3$ was obtained from the temperature dependence of the ^{99,101}Ru NMR peak frequencies (or HFs). Over the temperature range for which useable signal could be observed, $T \leqslant 21$ K, it was found that $\Delta\nu/\nu_0 = -AT^{3/2}$, where $A = 1.4 \times 10^{-4}$ K$^{-3/2}$. The characteristic Bloch law $T^{3/2}$ temperature dependence at low temperatures, which is indicative of spin-wave excitations being dominant, has been observed in other strong itinerant ferromagnets [26]. The distinction between the temperature dependence of the HF and the spontaneous magnetization has been discussed in detail by Dormann [17]. In the case where spin-wave excitations are dominant, the differences give rise to correction terms which are of higher order and will not be considered here. From standard spin-wave theory, the leading term in the fractional reduction of the spontaneous magnetization with temperature is

$$\frac{\Delta M_S}{M_{SO}} = -AT^{3/2} = -\left\{\frac{0.587}{SQ}\left(\frac{k_B}{2JS}\right)^{3/2}\right\}T^{3/2} \tag{6}$$

where $Q = 1$, 2 and 4 for simple-cubic, body-centred-cubic and face-centred-cubic lattices, respectively [27]. For $SrRuO_3$, the Ru atoms are in a (nearly) simple-cubic arrangement with each Ru atom being coupled to six other Ru atoms. Taking $A = 1.4 \times 10^{-4}$ K$^{-3/2}$ and assuming that $S = 1$, equation (6) yields a value of $J = 2.4$ meV for the exchange integral. For comparison, an approximate connection between J and the ordering temperature T_c can be obtained from mean field theory using

$$J = \frac{3k_BT_c}{2zS(S+1)} \tag{7}$$

where $z = 6$ is the number of neighbouring Ru moments. Equation (7) with $T_c = 160$ K for $SrRuO_3$ yields $J = 1.7$ meV, which is in good agreement with the value obtained from the temperature dependence of the spontaneous magnetization (HF).

In order to pursue further an understanding of the microscopic origin of the magnetic properties, NMR and muon spin rotation work is currently in progress on single crystal samples

of $Sr_{1-x}Ca_xRuO_3$ which do not possess any $SrRuO_3$ second phase. Although the NMR enhancement factor does not appear to be as favourable as for the polycrystalline samples, a similar decrease in the ^{99,101}Ru peak intensity is observed. Furthermore, the electric quadrupole effects, such as the spin-echo amplitude modulation, are more clearly resolved.

Acknowledgments

The authors wish to acknowledge the facilities, instrumentation and generous assistance of S E Brown at UCLA for some of the experimental work. Also, we are grateful to D M Pease for several useful discussions. The work at the University of Connecticut was supported by NSF grant DMR 9705136 (JIB, WAH and YDZ). The work at the University of California at Los Angeles was supported by NSF grant DMR 9705369 (WGC). The work at Brookhaven National Laboratory was supported by DOE grant DE-AC02-98-CH10886 (ARM).

References

[1] Bednorz J G and Müller K A 1986 *Z. Phys.* B **64** 189
[2] von Helmholt R, Wecker J, Holzapfel B, Schultz L and Samwer K 1993 *Phys. Rev. Lett.* **71** 2331
[3] Maeno Y, Hashimoto H, Yoshida K, Nishizake S, Fujita T, Bednorz J G and Lichtenberg F 1994 *Nature* **372** 532
[4] Callaghan A, Moeller C W and Ward R 1966 *Inorg. Chem.* **5** 1572
[5] Longo J M, Raccah P M and Goodenough J B 1968 *J. Appl. Phys.* **39** 1327
[6] Kanbayasi A 1978 *J. Phys. Soc. Japan* **44** 108
[7] Fumihiko F and Tsuda N 1994 *J. Phys. Soc. Japan* **63** 3798
[8] Randall J J and Ward R 1959 *J. Am. Chem. Soc.* **81** 2629
[9] Bouchard R J and Gillson J L 1972 *Mater. Res. Bull.* **7** 873
[10] Kobayashi H, Nagata M, Kanno R and Kawamoto Y 1994 *Mater. Res. Bull.* **29** 1271
[11] Cao G, McCall S, Shepard M, Crow J E and Guertin R P 1997 *Phys. Rev.* B **56** 321
[12] Klein L, Dodge J S, Ahn C H, Reiner J W, Mieville L, Geballe T H, Beasley M R and Kapitulnik A 1996 *J. Phys.: Condens. Matter* **8** 10 111
[13] Gibb T C, Greatrex R, Greenwood N N, Puxley D C and Snowdon K G 1974 *J. Solid State Chem.* **11** 17
[14] Zhang Y D, Budnick J I, Ford J C and Hines W A 1991 *J. Magn. Magn. Mater.* **100** 13 and references therein
[15] Clark W G, Hanson M E, Lefloch F and Ségransan P 1995 *Rev. Sci. Instrum.* **66** 2453
[16] Mims W B 1966 *Phys. Rev.* **141** 499
[17] Dormann E 1991 *Handbook on the Physics and Chemistry of Rare Earths* vol 14, ed K A Gschneidner and L Eyring (Amsterdam: Elsevier) p 63
[18] Cao G 1999 private communication
[19] *Magnetic Resonance Table* web site http://bmrl.med.uiuc.edu:8080mritable/
[20] Abe H, Yasuoka H and Hirai A 1966 *J. Phys. Soc. Japan* **21** 77
[21] Abragam A 1961 *The Principles of Nuclear Magnetism* (London: Oxford University Press) p 234
[22] Firestone R B 1996 *Tables of Isotopes* 8th edn, ed V S Shirley (New York: Wiley) pp 697, 731
[23] Ishida K, Kitaoka Y, Asayama K, Ikeda S, Nishizake S, Maeno Y, Yoshida K and Fujita T 1997 *Phys. Rev.* B **56** R505
[24] Carter G C, Bennett L H and Kahan D J 1977 *Metallic Shifts in NMR* part I (Oxford: Pergamon) p 316
[25] Mukuda H, Ishida K, Kitaoka Y, Asayama K, Kanno R and Takano M 1999 *Phys. Rev.* B **60** 12 279
[26] Argyle B E, Charap S H and Pugh E W 1963 *Phys. Rev.* **132** 2051
[27] Kittel C 1996 *Introduction to Solid State Physics* 7th edn (New York: Wiley)